

DNA - AN INTEGRATED OPEN-SOURCE OPTIMIZATION PLATFORM FOR THERMO-FLUID SYSTEMS

Leonardo Pierobon*, Jorrit Wronski, Brian Elmegaard and Fredrik Haglund
Technical University of Denmark
Department of Mechanical Engineering
2800 Kongens Lyngby
Denmark

Ian H. Bell
University of Liège
Thermodynamics Laboratory
4000 Liège
Belgium

ABSTRACT

This paper presents developments and new features added to the simulation tool Dynamic Network Analysis. This open-source software is the result of ongoing development at the Department of Mechanical Engineering, Technical University of Denmark since 1988. Ever since, it has been employed to model dynamic and steady-state energy systems and is now available for the most common operating systems (Windows, Mac OS and Linux). Emerging interest in novel plant technologies, high-temperature heat pumps, refrigeration absorption modules, and in energy system optimization has stressed the necessity to extend the capabilities of the software, while at the same time decreasing computational time. Dynamic Network Analysis can now solve non-convex optimization problems by virtue of the fully-embedded genetic algorithm. Moreover, the thermophysical fluid property library has been extended with more than 110 fluids by interfacing CoolProp, a high-accuracy open-source property package for pure and pseudo-pure fluids, as well as humid air. The new features are unveiled in one case study where the optimization of an air bottoming cycle unit recuperating the exhaust heat from an offshore power system is performed by taking advantage of CoolProp's table-based property interpolation scheme.

Keywords: DNA, CoolProp, Evolutionary algorithm, Thermophysical properties

NOMENCLATURE

a	Constants in Eq. 2 or air
F_h	Fin height [mm]
F_l	Fin length [mm]
h	Specific enthalpy [$\text{kJ} \cdot \text{kg}^{-1}$]
l_{exh}	Length gas side [m]
p	Pressure [bar]
T	Temperature [K]
v	Specific volume [$\text{m}^3 \cdot \text{kg}^{-1}$]
\bar{X}, \bar{Y}	Arrays of optimization variables
x, y	Tabulated and normalized fluid properties

Δ	Difference
ρ	Density [$\text{kg} \cdot \text{m}^{-3}$]

INTRODUCTION

Simulation of thermodynamic systems has become one of the main pillars of engineering work, university education as well as public and private research. Many software products are deeply integrated into existing workflows and increasing simulation quality has led to decreasing experimental efforts while accelerating the pace of implementation and development of new and optimised thermodynamic pro-

*Corresponding author: Phone: +45 254129 Fax: +45 884325 E-mail:lpier@mek.dtu.dk

cesses. Such processes involve a number of non-linear phenomena, e.g. the phase change of a working fluid or transitions between laminar and turbulent flow regimes, calling for robust solution strategies and integrators.

Software for modelling thermo-fluid systems typically involves an ecosystem of at least three interacting software components. First, a system interpreter (a) converts the users' input and creates a modified system of equations along with bindings to external libraries. These equations are then processed by a numerics component (b) containing solvers and integrators, which typically consist of custom-made special-purpose algorithms and modified versions of popular mathematics libraries like the Basic Linear Algebra Subprograms (BLAS) [1], its high-level companion the Linear Algebra Package (LAPACK) [2] and the Harwell Subroutine Library (HSL) [3]. The third component is the fluid property package (c) whose calculations are the bottleneck of the entire solving procedure while discontinuities in the thermophysical properties and their derivatives challenge the solvers' stability. For dynamic simulations, a fourth functional (d) unit can be introduced to provide access to data for varying operating conditions including controller inputs. Common software packages in the field of thermo-fluid simulations implement one or more of the four aspects, (a) through (d), mentioned above. If needed, missing features are often supplemented by accessing an independent library.

There are a number of software for steady-state simulation. Many customised solutions are based on the general purpose computing packages SciPy [4] and Matlab [5] exploiting their powerful solvers and data treatment facilities. A popular equation-based application for static modelling is the Engineering Equation Solver (EES) [6]. Another package for similar purposes is CycleTempo [7], which also comes with its own fluid property database, representing the component-based modelling environments. Dynamic problems formulated in systems of differential equations require other approaches such as the ones implemented in Ascend [8], AspenONE [9], Dynamic Network Analysis (DNA) [10] and the different implementations of the Modelica language, e.g. Dymola [11] and OpenModelica [12].

Fluid property calculations are usually delegated to external libraries that are accessed on a per-call ba-

sis extending a small group of built-in fluid property correlations. A commonly used library for this purpose is REFPROP [13] developed by the U.S. National Institute of Standards and Technology (NIST). It can handle pure and pseudo-pure fluids as well as a large amount of mixtures of common working fluids. Another commercial software for a similar purpose is FluidProp [14], the property calculation engine behind CycleTempo. Furthermore, the TIL Media Suite [15] provides access to optimised routines tailored for dynamic simulations.

The only freely-available high-accuracy property library for mixtures, known to the authors is TREND [16]. Both, TREND and CoolProp [17] are competitive free fluid property libraries for pure and pseudo-pure fluids since they contain a large selection of relevant working fluids with CoolProp offering the unique features of tabulated property interpolation. The other open-source alternatives FPROPS [18] from the Ascend project and the Modelica-based packages ModelicaMedia [19] and HelmholtzMedia [20] only have a limited number of working fluids. Currently, DNA includes its own routines for a number of fluids like water/steam by Wagner and Pruss [21] with LiBr-Water solutions added by Pátek and Klomfar [22], some real gases and mixtures of ideal gases [23], refrigerants [24]. It also contains functions for calculating properties of solid fuels such as biomass and coal. In particular, functions for thermal radiation properties of combustion products and exergy may be mentioned as uncommon features.

Looking at the above, integrating DNA with CoolProp combines a mature steady-state solver and integrator with a computationally efficient fluid property database. Due to the enhanced simulation speed, DNA can now be used to perform optimisation and control development tasks as described below.

DYNAMIC NETWORK ANALYSIS

The present section discloses new features and capabilities of the simulation tool Dynamic Network Analysis. Particular emphasis is dedicated to the newly implemented capabilities of solving multi-variable optimization problems and of utilizing advanced techniques for rapid computation of thermophysical and transport properties for a large variety of pure fluids.

New features

Dynamic Network Analysis is the present result of ongoing development at the Department of Mechanical Engineering, Technical University of Denmark, which began with a Master's Thesis work in 1988 [25]. DNA may be described as a modelling language for describing thermo-fluid systems and as the compiler that interprets this language and makes it accessible for the numerical solver. It can also provide some fluid property data and therefore covers the aforementioned components (a) and (c), while partly fulfilling tasks done by the numerics component (b). In DNA, the physical model is formulated analogously to electrical networks by connecting the relevant component models through nodes and by including operating conditions for the complete system. The physical model is converted into a set of equations to be solved numerically. The mathematical problem can include both dynamic and steady-state mass and energy conservation balances for all components and nodes, as well as relations for thermodynamic properties of the fluids involved. The program includes a component library with models for a large number of different components existing within energy systems.

DNA is an open source tool written in FORTRAN. It is integrated with the open source editor Emacs and the open source compiler suite GCC both distributed by the Free software Foundation [26].

DNA solves both steady state and dynamic problems. For steady state problems algebraic loops due to mass balances in thermodynamic cycles are detected and removed by the compiler. The solver is a modified Newton method.

Dynamics occur in mass and energy balances as well as in control algorithms and in inertia of rotating shafts. This results in differential-algebraic equations which are solved by a backward differentiation formulae (BDF) implemented for variable step size by use of the Nordsieck formulation. The solver handles discontinuities by restarting at the point of crossing.

The software capabilities are improved by linking DNA with the open-source genetic algorithm implemented by Carroll [27]. The code, readily available in Fortran language, is compiled together with DNA to form a unique software capable of solving non-convex optimization problems, to be set directly through the user interface. The genetic algorithm is

preferred to gradient-based methods since it is less prone to end its search in local minima of the problem, usually converging towards global optima. This comes at the cost of an increased computational effort, due to the large number of evaluations of the objective functions [28]. For a more in-depth description of the key features of the genetic algorithm employed in this work the reader can refer to Goldberg and Holland [29].

Additionally, the fluid library is extended with over 110 compressible fluids given as Helmholtz-free-energy-based equations of state (EOS) and over 50 incompressible liquids and solutions by using a custom-built C-interface to pass property calls to the open-source thermophysical property library CoolProp [17]. Furthermore, an integration with CoolProp also enables the usage of all fluids and mixtures available in REFPROP [13].

Matlab interface

Matlab is an important tool in many technical applications. It is used in control applications, often in combination with the Simulink tool. DNA has been demonstrated integrated with Matlab as a function that Matlab can call when needed to obtain data from the plant that the DNA model is emulating. This means that the complete DNA application more or less will be considered as a Simulink block with inputs and outputs. The inputs are control signals and the outputs are measurements one sampling time ahead, when DNA has calculated the new state. Matlab then may change to the control signals and run DNA again. The integration is implemented via the Matlab external interface (Mex) [30, 31]. One feature which has been wanted for the development of DNA as a Mex routine has been that it should run on both Microsoft Windows and Linux. For this reason GCC is used as compiler [32].

The algorithm used is:

```
Call Mexdna from Matlab with the DNA input file
as argument. The call is done via a Mex gateway
file.
```

```
Read the input file and initialize the DNA model
Return to Matlab
```

```
while Simulating do
```

```
Change boundary conditions for control signals,
load requirements and disturbances for the model.
```

```

Call Mexdna with sampling time step as input
Simulate until sampling time is reached
Return measurements (simulation results) to
Matlab
end while

```

To pass variables between Matlab and the external program, a gateway routine is required. This routine handles conversion between Matlab array pointers and the external types. In order to keep all variables in memory while the execution control is in Matlab, the persistent arrays feature is used.

Fluid properties

Nowadays, many engineering applications make heavy use of advanced mathematics to solve design and control problems. Especially iterative methods and differential equations involve numerous calls to the connected fluid property library. Hence, computational efficiency is of the utmost importance.

Helmholtz-free-energy-based equations of state (EOS) provide the most accurate source of thermodynamic data for many relevant working fluids [33]. However, evaluating state points to provide properties based on random inputs is a computationally expensive task. The EOS is usually provided in a temperature-density-explicit form and those two are not very common iteration variables for a simulation software. Interpolation methods can improve the speed of evaluation drastically. The described software uses two different interpolation methods: a) Tabular Taylor Series Expansion (TTSE) as described by Miyagawa and Hill [34] and Watanabe and Dooley [35] and b) bicubic interpolation published in the work of Keys [36]. To work efficiently, both methods require a regularly spaced grid of state points and a couple of derivatives with respect to the two independent variables.

The following examples illustrate the procedures employed to obtain the property values using the interpolation methods. Using TTSE, the temperature can be obtained from the often used inputs pressure

and enthalpy with the expansion

$$\begin{aligned}
T = & \Delta h \left(\frac{\partial T}{\partial h} \right)_p + \frac{\Delta h^2}{2} \left(\frac{\partial^2 T}{\partial h^2} \right)_p \\
& + \Delta p \left(\frac{\partial T}{\partial p} \right)_h + \frac{\Delta p^2}{2} \left(\frac{\partial^2 T}{\partial p^2} \right)_h \\
& + \Delta h \Delta p \left(\frac{\partial^2 T}{\partial p \partial h} \right) + T_{i,j}
\end{aligned} \quad (1)$$

where the derivatives are evaluated at the point i, j , and the differences are given by $\Delta p = p - p_i$ and $\Delta h = h - h_i$. The nearest state point can be found directly due to the regular spacing of the grid of points. For an improved representation of the p - v - T surface, bicubic interpolation can be used. In the bicubic interpolation method, the state variable and its derivatives are known at each grid point. This information is used to generate a bicubic representation for the property in the cell, which could be expressed as

$$T(x, y) = \sum_{i=0}^3 \sum_{j=0}^3 a_{ij} x^i y^j \quad (2)$$

where a_{ij} are constants based on the cell boundary values and x and y are normalized values for the enthalpy and pressure, for instance. The constants a_{ij} in each cell are cached for additional computational speed.

The increase in computational speed depends on the complexity of the EOS. Using IAPWS 1995[21] as an example for the properties of subcooled water at 10 MPa, both methods yield an acceleration by a factor of more than 120 for one of the most involved equations of state when calculating density from p and h based on the current implementation in Cool-Prop. The measured computational time of approximately 1 μ s per $\rho(p, h)$ -call is in good agreement with figures reported by Johansen [37] for the same fluid, which also provides an in-depth comparison of numerous interpolation schemes.

As another example of the accuracy of these interpolation methods, the density of air is evaluated at 40000 random data points covering the entire fluid surface. Figure 1 presents the results of this analysis. These data show that the accuracy of the bicubic interpolation method is generally several orders of magnitude better than that of the TTSE method, though both yield acceptable accuracy for most technical needs.

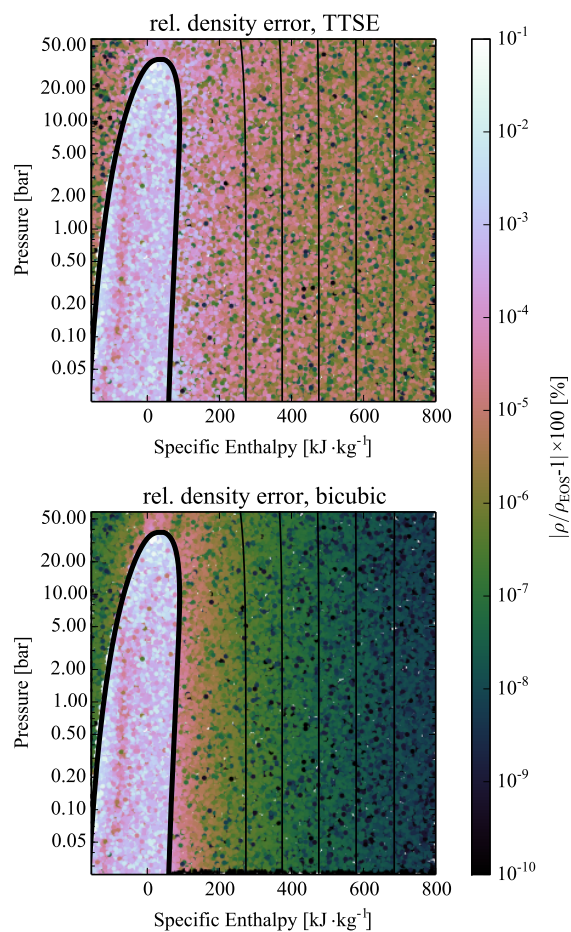


Figure 1: Interpolation errors for air from slightly above the triple point to 500 °C and 60 bar with isolines shown for 0 °C, 100 °C, 200 °C, 300 °C and 400 °C.

CASE STUDY

The work considers as exemplary application the power plant installed on the Draugen oil and gas offshore platform, located 150 km from Kristiansund, in the Norwegian Sea. The reservoir was discovered in 1984 and started operation in 1993. The platform, operated by A/S Norske Shell, produces gas exported via Åsgard gas pipeline to Kårstø (Norway) and oil, which is first stored in tanks at the bottom of the sea and then exported via a shuttle tanker (once every 1-2 weeks). The normal power demand is around 19 MW and it can increase up to 25 MW during oil export. To enhance the reliability and to diminish the risk of failure of the power system, two turbines run at a time covering 50 % of the load each, while the third one is kept on standby, allowing for maintenance work. Despite the low performance, this strategy ensures the necessary re-

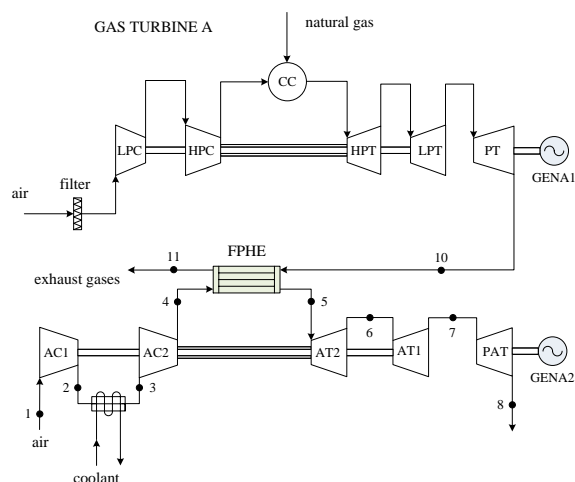


Figure 2: Simplified layout of the power system on the Draugen offshore oil and gas platform. Gas turbine B and C are not shown. The air bottoming cycle module recuperates part of the thermal power released with the exhaust gases of one engine, in the case gas turbine A.

serve power for peak loads, and the safe operation of the engines.

The system layout

Figure 2 shows the layout of the power system with the additional air bottoming cycle (ABC) module which recuperates the exhaust heat produced by gas turbine A. The engines B and C are not reported. Note that the bottoming cycle unit should have the capability to harvest the waste heat alternatively from the other two engines, thus ensuring high performances when switching the gas turbines on operation. The twin-spool engine employs two coaxial shafts coupling the low pressure compressor (LPC) with the low pressure turbine (LPT) and the high pressure compressor (HPC) with the high pressure turbine (HPT). The power turbine (PT) transfers mechanical power through a dedicated shaft to the electric generator (GEN). Natural gas is the fuel utilized in the combustion chamber (CC).

As regarding the ABC part, the first compressor (AC1) intakes ambient (1 → 2) air which then cools down in the intercooler (2 → 3), in this way diminishing the specific work during the compression process. The second compressor (AC2) increases further the pressure of the working fluid (3 → 4) which then harvests the exhaust energy from the gas turbine in the finned-plate heat exchanger (4 → 5). As reported in Kays and London [38], this device offers

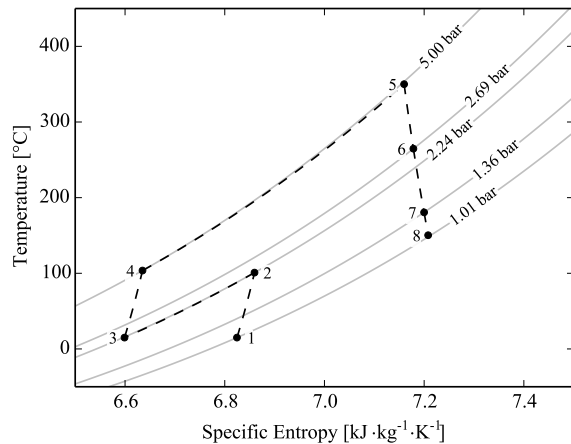


Figure 3: T - s diagram for the ABC unit (triple spool arrangement with one intercooler).

higher performances and compactness for gas-to-gas heat transfer processes compared to shell-and-tube and flat-plate heat exchangers. The air then expands through the air turbine AT2 (5 \rightarrow 6) which drives the second compressor, and afterwards through the air turbine AT1 (6 \rightarrow 7) which is mechanically connected to AC1. Finally, the power air turbine (PAT) produces useful power by driving the electric generator (7 \rightarrow 8).

Heat transfer equipment

The finned-plate heat exchanger serving the ABC power system consists of a stack of plates where the hot and cold fluids flow in the free space between the plates, typically in a cross flow arrangement, see Figure 4(a). The plates are equipped with a number of fins with the purpose of augmenting the surface area and of attaining larger heat transfer area-to-volume ratios, i.e. high compactness. The fins may have different shapes, e.g. wavy fins, offset fins and offset strip fins. The latter configuration (see Figure 4(b)) is the most widely adopted and it is thus the one selected in the current work. It is worth mentioning that FPHEs have to operate at lower temperatures (840 °C) and pressures (8.3 bar) [39] compared to shell-and-tube heat exchangers, depending on the process utilized to bond the metal plates. Given the boundary conditions for the ABC unit (see Table 2), these limitations are fulfilled in the present analysis.

The design approach to size the heat transfer equip-

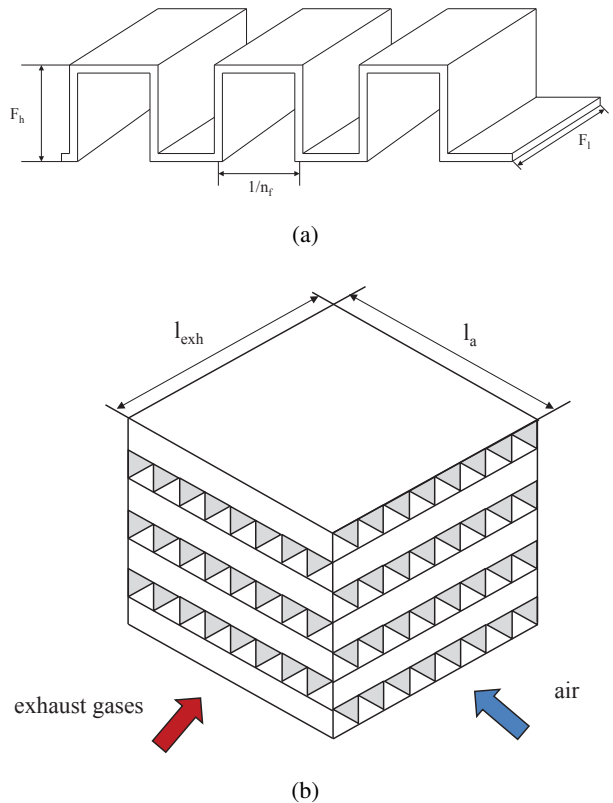


Figure 4: Layout of the finned-plate heat exchanger serving the air bottoming cycle power unit. 4(a) Exhaust gas and air flow pattern. 4(b) Detail of the fin pattern.

ment is the *effectiveness – NTU method* implemented as reported in Yousefi et al. [40]. The heat transfer coefficient and the pressure drop on each side of the finned-plate heat exchanger (see Figures 4(a) and 4(b)) are calculated in accordance to Manglik and Bergles [41]. The design model of the FPHE was verified by comparison with the geometrical data reported in Yousefi et al. [40]. The differences between the model results and the values reported in the references are within 4.0% in terms of both overall heat transfer coefficient and pressure drop.

The optimization problem

A feasible implementation of bottoming cycle units offshore requires to design compact and light modules, while at the same time exploiting the entire waste heat recovery potential. For this case study, the optimization problem is formulated in two main steps: i) find the cycle parameters maximizing the net power output of the ABC unit, and ii) define the

Table 1: Lower and upper bound for the variables involved in the optimization of the air bottoming cycle unit depicted in Figure 2.

Variable	Lower - upper bound
Outlet pressure p_2/p_1 [-]	1.2 - 3.2
Outlet pressure p_4/p_3 [-]	1.2 - 3.2
Fin height [mm]	50 - 200
Fin length [mm]	20 - 100
Gas side length [m]	1.0 - 3.0

geometry of the finned-plate heat exchanger which minimizes its weight given the optimal cycle variables.

The genetic algorithm carries out the two tasks by acquiring the array of the parameters and the upper and lower bounds limiting the possible values for the vectors of the optimization variables \bar{X} and \bar{Y} , which read

$$\bar{X} = \left[\frac{p_2}{p_1}, \frac{p_4}{p_3} \right] \text{ and} \quad (3)$$

$$\bar{Y} = [F_{h,a}, F_{l,a}, F_{h,exh}, F_{l,exh}, l_{exh}] . \quad (4)$$

In Equation 3, p_2/p_1 and p_4/p_3 are the pressure ratios of the two air compressors, see Figure 2. The variables F_h , F_l and l_{exh} are the fin height, the fin length and the length of the exhaust gas side. The subscripts "a" and "exh" refer to the air and the exhaust stream side.

The objective functions for steps i) and ii) are the electric power output of the generator serving the ABC unit and the weight of the finned-plate heat exchanger calculated from the design analysis. Table 1 lists the upper and lower bounds of the optimization variables. Note that the values related to the geometry of the heat exchanger are set accordingly with the figures reported in Shah and Sekulić [39] and Yousefi et al. [40].

Table 2 lists the parameters which are maintained constant during the two successive optimizations. As the use of integer variables in the optimization routine is beyond the capabilities of the algorithm, the fin per meter and the number of plates are kept constant. The thickness of the finned-plate heat exchanger and the construction material (stainless steel) are retrieved from Bolland et al. [42].

As the gas turbine can operate on a wide range of both liquid and gaseous fuels, the terminal temper-

Table 2: Parameters assumed for the two-step optimization.

Parameter	Value
Generator efficiency [%]	98
Ambient temperature [°C]	15
Ambient pressure [bar]	1.013
Gas turbine	
Electric power output [MW]	16.524
Thermal efficiency [%]	31.3
Exhaust gas temperature [°C]	379.2
Exhaust gas mass flow [kg · s ⁻¹]	91.5
Air bottoming cycle unit	
Water inlet temperature [°C]	5
Water outlet temperature [°C]	40
Pressure drops air side [bar]	0.03
Outlet temperature t_5 [°C]	330
Exhaust temperature t_{11} [°C]	160
Compressor mechanic efficiency [%]	99.8
Compressor isentropic efficiency [%]	86
Turbine isentropic efficiency [%]	90
Finned-plate heat exchanger	
Fins per meter air side [m ⁻¹]	500
Fins per meter gas side [m ⁻¹]	500
Number of plates [-]	60
Fin thickness [μm]	200
Plate thickness [μm]	200

ature of the exhaust gases exiting the FPHE is set to 160 °C. This precaution prevents condensation of corrosive compounds when fuels such as crude oil, heavy fuel oil and naphtha are combusted. In the geometric optimization of the finned-plate heat exchanger it is verified that the velocity on the hot and cold side of the heat exchangers is within 1 m · s⁻¹ and 40 m · s⁻¹, while an upper limit of 3 kPa is selected for the pressure drops. If such test is not passed the objective function is set to a large number, i.e. 10⁶.

The parameters of the genetic algorithm are specified according to De Jong and Spears [43]: generation size 1000, crossover rate 0.6, and mutation rate 0.001. As for the population number in the first optimization and in the weight minimization, the specified values are 5 and 50, respectively. These numerical quantities are selected so as to ensure the repeatability of the solution when different simulations are performed. The process terminates when the average change in the objective function of two succes-

sive iterations is lower than the specified tolerance (10^{-4}) or when the number of generation reaches the maximum value.

RESULTS

Figure 5 shows the optimal value of the objective function, i.e. the net power output of the ABC module, at each generation for the optimization of the thermodynamic cycle. The electric power remains between 2730 kW and 2750 kW for the first 180 generations. The largest improvement is attained at generation 179 where the objective function reaches a value of 2756 kW. Considering the first generation as a reference, the total gain in power across the optimization process is around 30 kW which corresponds to a relative improvement of 1.1 %.

Figure 6 reports the value of the optimization variables, i.e. the pressure ratios of the two air compressors, as a function of the generation number. Accordingly with the trend of the objective function, the pressure ratios reach the best values, i.e. 1.685 and 2.543, after 340 generations. The final quantities differ from the ones of the first generation by 8.1 % and 3.7 %, respectively.

Figure 7 reports the evolutionary trend of the weight of the finned-plate heat exchanger for the second optimization. It is underlined that the pressure ratios of the compressors are now fixed to the optimal values. It can be noted that the algorithm employs all the available generations to abate the value of the objective function. The largest improvements occur during the first ten generations where the target parameter decreases from $40 \cdot 10^3 \cdot \text{kg}$ to $35 \cdot 10^3 \cdot \text{kg}$.

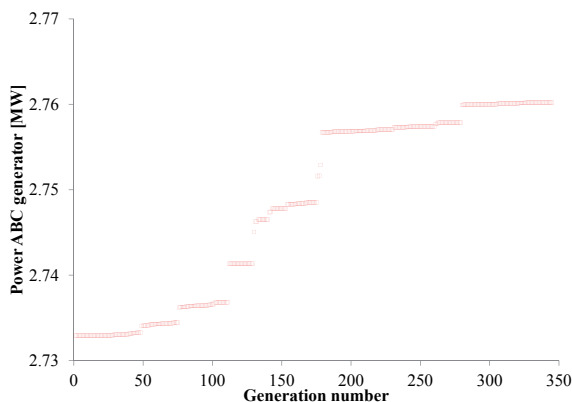


Figure 5: Maximum value of the object function (net power output) for each generation number of the air bottoming cycle optimization.

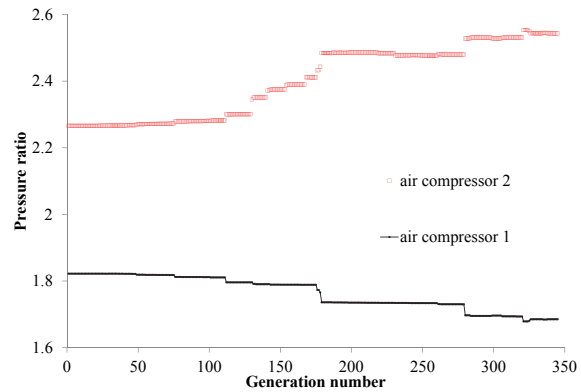


Figure 6: Best values of the optimization variables (see Equation 3) for each generation number of the air bottoming cycle optimization.

Smaller weight decrements can be found during iteration number 210 and 870. The final value of the objective function is $33.8 \cdot 10^3 \cdot \text{kg}$.

Figure 8 shows the evolutionary trend of one optimization variable, i.e. the fin height on the exhaust gas side, involved in the routine. The largest variations occur during the very first evolutions where the fin height of the exhaust gas side diminishes from 75.5 to 84.7 mm. The last variation ($\approx 1.0 \text{ mm}$) occurs at iteration number 846.

Table 3 lists the results of the two-steps optimization of the ABC power system. The thermal efficiency of the ABC unit (12.6 %) is calculated as the ratio between the electric power output and the heat rate exchanged by the FPHE.

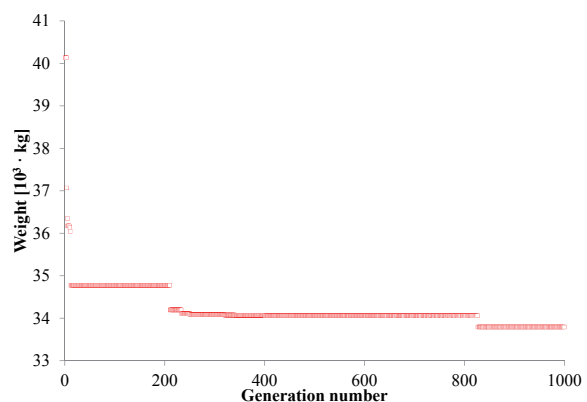


Figure 7: Maximum value of the object function (weight) for each generation number of the finned-plate heat exchanger optimization.

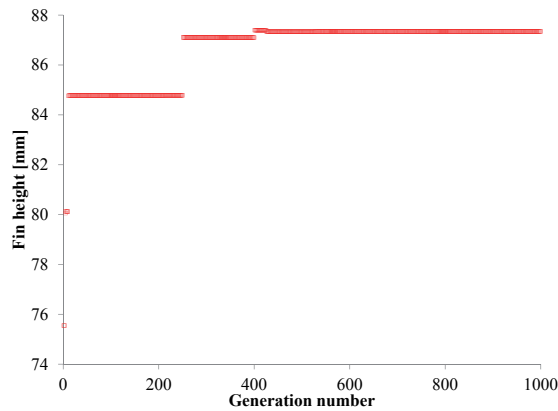


Figure 8: Best value of the fin height on exhaust gas side (see Equation 4) for each generation number of the weight optimization.

Table 3: Results of the two-step optimization. Air bottoming cycle unit and finned-plate heat exchanger design.

Parameter	Value
Air bottoming cycle	
Pressure ratio p_2/p_1 [-]	1.685
Pressure ratio p_4/p_3 [-]	2.543
Net power output [MW]	2.76
Thermal efficiency [%]	12.6
Finned-plate heat exchanger	
Fin height air side [mm]	80.5
Fin length air side [mm]	30.8
Fin height gas side [mm]	87.3
Fin length gas side [mm]	66.5
Gas side length [m]	1.43
Effectiveness [%]	86.9
Heat transfer area [m ²]	20463
UA-value [kW · m ⁻² · K ⁻¹]	90.3
Core volume [m ³]	42.0
Total weight [10 ³ · kg]	33.8

DISCUSSION

As for the optimization of the ABC system, the power output and the thermal efficiency of the plant illustrated in Figure 2 increase from 16.5 MW to 19.3 MW and from 31.3 % to 36.5 %, respectively. Hence, for the thermal efficiency an increment of 5.2 %-points is attained. The improvement appears to be smaller than the values reported in the open literature. For example, Tveitaskog and Haglind [44] report an increment of around 10.5 %-points for the LM2500 gas turbine, and Poullikkas [45] estimates an improvement of the net power output of the Al-

lison 571-K engine from 5.9 MW to 7.5 MW, corresponding to an increment of 27.0 %. The lower gains obtained here are due to two reasons. Firstly, the SGT-500 machine exhibits a colder exhaust gas temperature (379.2 °C) compared to the gas turbines investigated in the aforementioned works. Thus, smaller increments are to be expected due to the lower attainable efficiency of the bottoming cycle. Furthermore, this work assumes conservative values for the temperature of the exhaust gases and at the inlet of the first air turbine so as to account for a reasonable size of the primary heat exchanger and to preserve the fuel flexibility of the topping unit. Operating gas turbines at lower temperatures effectively reduces corrosion caused by impurities in the fuel as well as the deposition of ashes [46].

As for the heat exchanger calculations, the values listed in Table 3 are in accordance, considering the different size of the plants, with the values obtained by Bolland et al. [42] for the design of a finned-plate heat exchanger of a ABC module recuperating the exhaust heat from the LM2500 gas turbine.

As reported in the previous section, the genetic algorithm computes the optimal pressure ratios of the two air compressors in 345 generations, given the boundary conditions listed in Table 2. Figure 9 shows a contour plot which highlights the impact of the two optimization variables on the net power output of the air bottoming cycle unit. The dark-red zones are characterized by low net power outputs, while the white ones define the regions of high values for the target function. The outcomes of the first optimization step are in-line with the results of such sensitivity analysis since the optimal pressure ratios lay in the white area of Figure 9.

To be noted that the first optimization handles a convex quadratic function with positive definite Hessian, see Figure 9. Under these hypothesis gradient-based approaches such as the steepest descent method are ensured to detect the exact solution with high rates of convergence and with a fixed number of iterations. These properties are expected to be poorer for the genetic algorithm due to the stochastic approach and depending on the input parameters, e.g. populations size, mutation rate.

The benefits of evolutionary approaches are instead fully exploited when minimizing the weight of the finned-plate heat exchanger. In fact, the second optimization process has to deal with numerous discon-

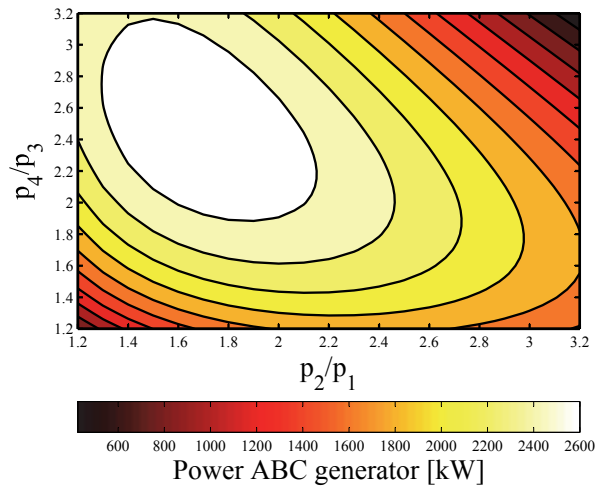


Figure 9: Contour plot showing the impact of the pressure ratios of the air compressors on the net power output of the air bottoming cycle unit.

tinuities in the objective function, which arise when the solver hits the limitations of the velocity and of the pressure drops in the FPHE. Figure 10 shows the effect of variations in the height and length of the fins installed on the air side. The figures for the remaining three variables are kept at the optimal values listed in Table 3.

In this case the white zones indicate regions where infeasible designs are attained as the pressure drops or fluid velocities exceed the predefined limits. Since in these cases the objective function is set to an arbitrary value (10^6), the bounds create discontinuities which can be promptly handled by the genetic algorithm. Moreover, stochastic methods are in this case preferable by virtue of the non-convexity of the target function, making gradient-based methods largely dependent on the starting point and more prone to convergence issues.

OUTLOOK AND CONCLUSIONS

Fluid Properties

In order to employ the interpolation techniques discussed above, tabulated data has to be generated from the EOS. The current implementation uses gridded data sets in terms of enthalpy h and logarithmic pressure $\log p$ and logarithmic specific volume $\log v$ and temperature T , respectively. The minimum enthalpy h_{\min} is the enthalpy of the saturated liquid state at the minimum temperature defined by

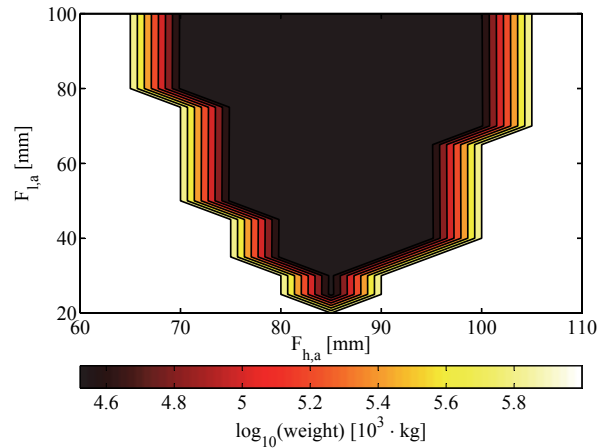


Figure 10: Contour plot showing the impact of the height and length of the fins installed on the air side on the weight of the finned-plate heat exchanger.

the employed EOS T_{\min} . The enthalpy difference between saturated liquid and saturated vapour at T_{\min} is added twice to h_{\min} yielding h_{\max} . The minimum pressure p_{\min} is defined by the saturated vapour state at T_{\min} . p_{\max} is obtained from multiplying the reducing pressure of the EOS (often the critical pressure) with two. T_{\max} is defined in the same way, while minimum and maximum specific are extracted from the previously generated tables in h and $\log p$. The regularly spaced grids are shown in Figure 11. It is obvious from Figure 11, that the two ranges of tabulated data do not cover the same regions. Therefore, additional calculation steps are required to assure that the calculation stays within the bounds of both data sets.

Due to the high accuracy of the interpolation methods shown in Figure 1, the next version of CoolProp will cover the whole T, p and h, p space for an EOS with the same amount of data points. Maximum enthalpy is obtained from T_{\max} in the low pressure limit. Besides the obvious boundaries given by T, p and h, p , a melting curve based on the Simon-Glatzel equation can be used to further reduce the application of the interpolation schemes. Special cases like with a negative inclination of the melting curve in h, p coordinates, like water, still require the evaluation of the EOS in some cases. With those two data sets, a one-dimensional search in the tables allows for twelve different input pairs. Only the combinations s, u and s, v and u, v will not be covered. Transport properties will be tabulated in T, p with numerical derivatives instead of T, v to play well together

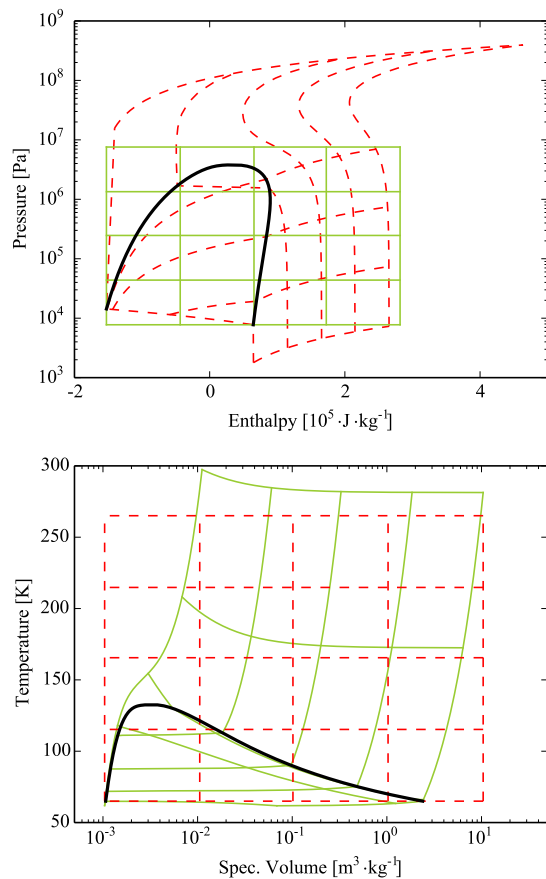


Figure 11: Interpolation tables in h, p (solid) and v, T (dashed) as generated by CoolProp v4.

with the other tabulated data.

Modelling and Optimisation

This paper discloses new features and capabilities of the open-source simulation program Dynamic Network Analysis developed at the Technical University of Denmark.

The tool has been interfaced to the open-source thermophysical property library Coolprop. The user can now model novel energy system technologies by leveraging the extended fluid library which includes more than a hundred compressible and incompressible fluids. Rapid and accurate calculations of thermodynamic and transport properties are delivered by virtue of advanced interpolation methods, i.e. tabular Taylor series expansion and bicubic interpolation. Moreover, Dynamic Network Analysis can deal with non-convex multi-variable optimization problem utilizing the fully embedded genetic

algorithm.

The new features are here exploited to design an air bottoming cycle module to recuperate the exhaust heat from the gas turbine-based power system installed on an oil and gas facility in the Norwegian Sea. Optimizing the pressure ratios of the two air compressors evidences opportunities for improvements in efficiency and installed power capacity of 5.2 %-points and 2.76 MW, respectively. Furthermore, the application of the genetic algorithm enables to minimize the compactness and the weight of the heat transfer equipment of around $6.2 \cdot 10^3 \cdot \text{kg}$. The full potential of the evolutionary algorithm is exploited in the latter optimization owing to the large discontinuities in the objective function.

Closing Remarks

From a broader perspective, the implemented routines, returning the physical properties of real fluids and optimal plant designs delivered in an open-source environment, constitute essential features to tackle the modelling challenges posed by future energy system in a computationally efficient and accurate way.

REFERENCES

- [1] C L Lawson, R J Hanson, D R Kincaid, and F T Krogh. Basic linear algebra subprograms for fortran usage. *ACM Transactions on Mathematical Software*, 5(3):308–323, September 1979.
- [2] E Anderson, Z Bai, C Bischof, S Blackford, J Demmel, J Dongarra, J Du Croz, A Greenbaum, S Hammarling, A McKenney, and D Sorensen. *LAPACK Users' Guide*. Society for Industrial and Applied Mathematics, Philadelphia, PA, third edition, 1999. ISBN 0-89871-447-8.
- [3] Scientific Computing Department and UK Science and Technology Facilities Council. HSL – A collection of Fortran codes for large scale scientific computation, 2013. URL <http://www.hsl.rl.ac.uk>.
- [4] E Jones, T Oliphant, P Peterson, et al. SciPy: Open source scientific tools for Python, 2001.

- URL <http://www.scipy.org/>. [Online; accessed 2014-08-04].
- [5] The MathWorks. Matlab R2013b, 2013.
- [6] Sanford Klein and F L Alvarado. *EES – Engineering Equation Solver v9.616*. F-Chart Software, Madison, Wisconsin, USA.
- [7] Asimptote bv and Propulsion and Power group at Delft University of Technology. Cycle-Tempo, 2014. URL <http://www.asimptote.nl/software/cycle-tempo>.
- [8] B Allan, K Chittur, L Cisternas, J Pye, V Rico-Ramirez, J Shao, J St Clair, M Thomas, A Westerberg, and D Coffey. ASCEND modelling environment v4, 2014. URL <http://ascend4.org>.
- [9] Aspen Plus. Release AspenONE, Aspen Technology. Inc., Cambridge, MA, USA, 2004.
- [10] B Elmegaard and N Houbak. DNA—a general energy system simulation tool. In *Proceedings of SIMS 2005*, pages 1–10, Trondheim, Norway, October 2005.
- [11] Dassault Systèmes AB. Dymola 2014. Lund, Sweden, 2013.
- [12] Open Source Modelica Consortium. OpenModelica, 2014. URL <https://openmodelica.org>.
- [13] E W Lemmon, M L Huber, and M O McLinden. NIST Standard Reference Database 23: Reference Fluid Thermodynamic and Transport Properties-REFPROP, Version 9.0, 2010.
- [14] Asimptote bv and Propulsion and Power group at Delft University of Technology. FluidProp v3.0, 2014. URL <http://www.fluidprop.com>.
- [15] TLK Thermo GmbH. TIL Media Suite, 2014. URL <http://www.tlk-thermo.com>.
- [16] R Span, T Eckermann, J Gernert, S Herrig, A Jäger, and M Thol. TREND – Thermodynamic Reference and Engineering Data v1.1, 2014. URL <http://www.thermo.rub.de>. Lehrstuhl für Thermodynamik, Ruhr-Universität Bochum.
- [17] I H Bell, J Wronski, S Quoilin, and V Lemort. Pure and pseudo-pure fluid thermophysical property evaluation and the open-source thermophysical property library CoolProp. *Industrial & Engineering Chemistry Research*, 53(6):2498–2508, 2014.
- [18] J Pye, S Muratet, K Chittur, H Ke, R Towers, S Ranganadham, and A Mittal. FPROPS, 2014. URL <http://ascend4.org/FPROPS>.
- [19] H Tummescheit, J Eborn, F J Wagner, M Otter, M Tiller, H Elmqvist, H Olsson, S E Mattsson, and K Pröß. Modelica.Media v3.1, 2013. URL <http://modelica.github.io/Modelica/om/Modelica.Media.html>. Modelica Association.
- [20] M Thorade. HelmholtzMedia – A fluid properties library, 2014. URL <https://github.com/thorade/HelmholtzMedia>.
- [21] W Wagner and A Pruss. The IAPWS Formulation 1995 for the Thermodynamic Properties of Ordinary Water Substance for General and Scientific Use. *Journal of Physical and Chemical Reference Data*, 31:387–535, 2002.
- [22] J Pátek and J Klomfar. A computationally effective formulation of the thermodynamic properties of LiBr-H₂O solutions from 273 to 500 K over full composition range. *International Journal of Refrigeration*, 29(4):566–578, June 2006.
- [23] B Lorentzen. *Power Plant Simulation*. PhD thesis, Technical University of Denmark, Laboratory for Energetics, 1995.
- [24] M J Skovrup. Thermodynamic and thermophysical properties of refrigerants – package in borland delphi for the refrigerants. Technical Report Version 3.10, Technical University of Denmark, October 2001.
- [25] C Perstrup. Analysis of power plant installation based on network theory. Master’s thesis, Technical University of Denmark, Laboratory of Energetics, 1991.

- [26] "Free Software Foundation". The free software directory, 2014. URL <http://www.fsf.org/>.
- [27] D L Carroll. D.L. Carroll's FORTRAN Genetic Algorithm Driver, November 1998. URL http://read.pudn.com/downloads47/sourcecode/others/158036/ga170.f__.htm.
- [28] K Deb. *Multi-objective optimization using evolutionary algorithms*, volume k. John Wiley & Sons, Inc., West Sussex, Great Britain, 2001.
- [29] D E Goldberg and J H Holland. Genetic algorithms and machine learning. *Machine learning*, 3(2):95–99, 1988.
- [30] MathWorks. *External Interfaces – version 6*. The MathWorks, <http://www.mathworks.com>, . Introduction of mex, downloaded May 27, 2004.
- [31] MathWorks. *External Interfaces Reference – version 6*. The MathWorks, <http://www.mathworks.com>, . Reference of mex and mx functions, downloaded May 27, 2004.
- [32] M Brett. *Compiling Matlab mex files with gcc for Windows*. <http://gnumex.sourceforge.net/>, wed dec 3 18:42:22 pst 2003 edition, 2003. Documentation of gnumex, downloaded May 28, 2004.
- [33] R Span, W Wagner, E W Lemmon, and R T Jacobsen. Multiparameter equations of state—recent trends and future challenges. *Fluid Phase Equilibria*, 183:1–20, 2001.
- [34] K Miyagawa and P G Hill. Rapid and accurate calculation of water and steam properties using the tabular Taylor series expansion method. *Journal of Engineering for Gas Turbines and Power*, 123(3):707–712, 2001.
- [35] K Watanabe and R B Dooley. Guideline on the Tabular Taylor Series Expansion (TTSE) Method for Calculation of Thermodynamic Properties of Water and Steam Applied to IAPWS-95 as an Example. Technical report, The International Association for the Properties of Water and Steam, Vejle, Denmark, August 2003.
- [36] R G Keys. Cubic convolution interpolation for digital image processing. *Ieee Transactions On Acoustics, Speech, And Signal Processing*, 29(6):1153–1160, 1981.
- [37] A O Johansen. *Numerical study of evaporators in power plants for improved dynamic flexibility*. Phd thesis, Technical University of Denmark, 2013.
- [38] W M Kays and A L London. *Compact heat exchangers*. McGraw-Hill, New York, United States of America, 1984.
- [39] R K Shah and D P Sekulić. *Fundamentals of Heat Exchanger Design*. John Wiley & Sons, Inc., Hoboken, United States of America, 2003.
- [40] M Yousefi, R Enayatifar, and A N Darus. Optimal design of plate-fin heat exchangers by a hybrid evolutionary algorithm. *International Communications in Heat and Mass Transfer*, 39(2):258–263, 2012.
- [41] R M Manglik and A E Bergles. Heat transfer and pressure drop correlations for the rectangular offset strip fin compact heat exchanger. *Experimental Thermal and Fluid Science*, 10(2):171–180, 1995.
- [42] O Bolland, M Forde, and B Hånde. Air bottoming cycle: use of gas turbine waste heat for power generation. *Journal of engineering for gas turbines and power*, 118:359–368, 1996.
- [43] K A De Jong and W M Spears. An analysis of the interacting roles of population size and crossover in genetic algorithms. In *Parallel Problem Solving from Nature*, volume 496 of *Lecture Notes in Computer Science*, pages 38–47. Springer Berlin Heidelberg, 1991.
- [44] K A Tveitaskog and F Haglind. Optimization of advanced liquid natural gas-fuelled combined cycle machinery systems for a high-speed ferry. In *Proceedings of ASME Turbo Expo 2012*, pages 329–338, Copenhagen, Denmark, June 2012.
- [45] A Poullikkas. An overview of current and future sustainable gas turbine technologies. *Renewable and Sustainable Energy Reviews*, 9(5):409–443, 2005.

- [46] F Haglind. A review on the use of gas and steam turbine combined cycles as prime movers for large ships. part iii: Fuels and emissions. *Energy Conversion and Management*, 49(12):3476–3482, 2008.